FAULTING AS AN EXPRESSION OF PLANETARY-TYPE PROCESSES ON VESTA. J. E. C. Scully[1], C. T. Russell[1], A. Yin[1], T. J. Bowling[2], [1]Department of Earth, Planetary, and Space Sciences, University of California, Los Angeles, 595 Charles Young Drive East, Box 951567, Los Angeles, CA 90095-1567, USA (jscully@ucla.edu), [2]Department of Earth, Atmospheric, and Planetary Sciences, Purdue University, 550 Stadium Mall Drive, West Lafayette, IN 47907, USA.

Introduction: The Dawn spacecraft orbited Vesta (mean diameter of ~525 km) from 2011 to 2012. Vesta is the second most massive asteroid in the asteroid belt and differentiated ~4.56 bya to form a core, a mantle and a crust [e.g. 1, 2]. Vesta is an intact protoplanet that exhibits many planetary-type processes [e.g. 3]. For example, the surface has a diversity of processes and compositions, which are reminiscent of planetary surfaces. There are separate terrains and geologic units [e.g. 4]; and pitted terrain [5], curvilinear gullies and lobate deposits [6] form in processes analogous to those on Mars and Earth. There is also surface compositional heterogeneity, in the form of exogenous carbonaceous chondrite [7, 8], hydrated minerals [9, 10] and olivine [11]. Large-scale faulting (~460 km long) has been induced by the largest impacts on Vesta. This large-scale faulting is another example of planetary-type processes, and is the focus of our work.

Background and previous work: Geometrical relationships [12, 13], numerical modeling [14], and impact experiments [15] find that formation of the Veneneia impact basin (diameter ~450 km) in the southern hemisphere induced the formation of the Saturnalia Fossae (460 km long) in the northern hemisphere; and that formation of the Rheasilvia impact basin (diameter ~500 km) in the southern hemisphere induced the formation of the Divalia Fossae (465 km long) in the equatorial regions. The fossae are interpreted as graben and half-graben [12-16]. The Saturnalia Fossae have recently been mapped in detail [16].

Methods: We build upon the work of [12-16] by use of highest resolution Dawn Framing Camera clear filter images (~20 m/pixel) [17]. We also utilize the highest resolution shape model (~50 m/pixel), derived from the Framing Camera images via stereophotoclinometry [18]. We use ESRI ArcMap 10 software to map in two-dimensions. In addition, we use ESRI ArcMap 10 and the USGS ISIS software to produce profiles and oblique surface views, which allow for three-dimensional analysis.

Results:

Saturnalia Fossae: observations and interpretations. Since the publication of [16], the highest resolution shape model has been produced. This allows us to define the morphology of the Saturnalia Fossae in more detail. We find that Saturnalia Fossa A is the dominant structure (460 km long, 52 km maximum width, 3.75 km maximum depth), and interpret it as a graben. Saturnalia Fossae B – E are smaller structures (110-450 km long, 6-18 km wide, 0.75-2.25 km deep), and we interpret them as half-graben. We find that all the Saturnalia Fossae are highly modified; they have low sharpness and distinctiveness, and are highly smoothed and rounded.

Divalia Fossae: observations and interpretations. Previous studies found the Divalia Fossae consist of a dominant structure and multiple smaller scale fossae, interpreted as graben and half-graben [13, 19]. We call the dominant structure Divalia Fossa A (465 km long, 22 km maximum width, 3.5 km maximum depth), and interpret it as a graben. We identify ~15 smaller scale fossae (90-490 km long, 11-14 km wide, 1.25-1.75 km deep) and interpret them as half-graben and graben. We find that the Divalia Fossae are less modified than the Saturnalia Fossae; they have moderate sharpness and distinctiveness, are moderately smoothed and less rounded than the Saturnalia Fossae.

Comparison with numerical modeling. Numerical modeling of the formation of the fossae uses a simplified Vesta, and simplified impact conditions [14]. Thus, we assess the applicability of this model to the real effects of the impacts by comparison with our geologic observations and interpretations.

The model predicts that the Divalia Fossae formed by impact-induced extensional strain and right-lateral shear strain in the top couple of kilometers of the crust [14]. Extension forms two conjugate normal faults that down-drop a central block to form an ~E-W oriented graben. Right-lateral shear strain induces bookshelf-type normal faulting, where the faults tilt to the north. ~E-W oriented half-graben form on top of the blocks. Our geologic observations and interpretations of the Divalia Fossae show ~E-W oriented graben and ~E-W oriented half-graben, formed by northerly dipping faults. Thus, they are consistent with the model.

The Saturnalia Fossae are proposed to form in a similar process [14]. Our geologic observations and interpretations of the Saturnalia Fossae do show a ~E-W oriented graben and ~E-W trending half-graben. However, the half-graben are interpreted to form as a result of southerly dipping faults, which is inconsistent with the model. While the results of the model are broadly consistent with the geologic observations and interpretations, further analysis of the inconsistency

may lead to a fuller understanding of the formation and/or modification processes of the fossae.

Discussion and conclusions:

Why do Saturnalia and Divalia Fossa A have similar lengths and depths? Maximum displacement (D) to length (L) ratios for faults scale with gravity [e.g. 20]. For example, D : L ratios of faults in basalts on Earth and Mars become smaller with decreasing gravity [20]. Using fossae depth as a proxy for apparent maximum displacement, we plot D : L ratios of the Vestan fossae on a plot of D : L ratios of faults on Earth and Mars, taken from [20] (see Figure). Faults in essentially basaltic material on Earth, Mars and Vesta plot along a roughly linear trend, and follow the pattern of decreasing D : L ratios with decreasing gravity. Thus, we propose that the lengths and depths of the fossae are similar because the sizes of these attributes are controlled by the low gravity of Vesta (~0.25 m/s^2).

Why do the fossae have different states of modification? Crater size-frequency distributions are used to derive absolute age estimates of the fossae, via an asteroid-flux-derived chronology system [21-23] and via a lunar-derived chronology system [4, 24]. Both chronology systems find that the Saturnalia Fossae are relatively older than the Divalia Fossae. We estimate that the regolith around the Saturnalia Fossae is >/≈5.2 km deep, and >/≈4.4 km deep around the Divalia Fossae. We propose that the Saturnalia Fossae are more modified than the Divalia Fossae because the Saturnalia Fossae are older, have a greater crater density, a greater regolith thickness and greater amounts of mass wasting of regolith than the Divalia Fossae. All these processes contribute to make the Saturnalia Fossae less sharp, more smoothed and more rounded than the Divalia Fossae.

Why do Saturnalia Fossa A and Divalia Fossa A have different widths? The widths of the fossae approximate the spacing between the normal faults that form the fossae. Spacing of faults is inversely controlled by the density of the material in which they form [e.g. 25], and fault spacing is directly controlled by the thickness of the faulted layer [e.g. 26, 27]. Therefore, we propose that Saturnalia Fossa A is more widely spaced than Divalia Fossa A because the faults forming Saturnalia Fossa A occur in a less dense material and/or because they occur in a thicker faulted layer. Our estimate of a thicker regolith around the Saturnalia Fossae is consistent with this proposition.

Why are the fossae a planetary-type process? The fossae were first proposed to form on Vesta because Vesta's differentiated interior amplified the impact-induced stresses, which would not occur on smaller, non-differentiated bodies [13]. Furthermore, numerical modeling of an impact into a differentiated Vesta confirms that a differentiated interior is necessary to form the fossae [e.g. 14]. In addition, the form and scale of the fossae are more similar to large-scale impact induced faulting features on rocky planets and moons [e.g. 28, 29], than the small-scale impact induced fractures on asteroids such as Eros and Lutetia [e.g. 30, 31]. Finally, the lengths, depths and widths of the fossae appear to be controlled by the same processes that control these attributes on rocky planets.

In summary, all these characteristics strongly indicate that the Vestan fossae are another example of the planetary-type process that occur on Vesta. Moreover, since the formation of the fossae requires a differentiated and relatively undisturbed interior, the presence of the fossae is further evidence that Vesta is an intact protoplanet.

References: [1] McSween, H.Y., et al. (2011) *Space Sci. Rev., 163,* 141-174. [2] Russell, C.T., et al., (2012) *Science, 336,* 684-686. [3] Russell, C.T., et al. (2014) *Eur. Planet. Sci. Congress*, 18. [4] Yingst, R.A., et al. (2014) *Planet. Space Sci., 103,* 2-23. [5] Denevi, B.W., et al. (2012) *Science, 338,* 246-249. [6] Scully, J.E.C., et al. (2015) *Earth Planet. Sci. Lett., 411,* 151-163. [7] McCord, T.B., et al. (2012) *Nature, 491,* 83-86. [8] Reddy, V., et al. (2012) *Icarus, 221,* 544-559. [9] De Sanctis, M.C., et al. (2012) *Astro. J. Lett., 758,* L36. [10] Prettyman, T.H., et al. (2012) *Science, 338,* 242-246. [11] Ammannito, E., et al. (2013) *Nature, 504,* 122-125. [12] Jaumann, R., et al. (2012) *Science, 336,* 687-690. [13] Buczkowski, D.L., et al. (2012) *Geophys. Res. Lett., 39,* L18205. [14] Bowling, T.J., et al. (2014) *Vesta in the Light of Dawn,* 2018. [15] Stickle, A.M., et al. (2015) *Icarus, 247*, 18-34. [16] Scully, J.E.C., et. al. (2014) *Icarus, 244,* 23-40. [17] Sierks, H., et al. (2011) *Space Sci. Rev., 163,* 263-327. [18] Gaskell, R., et al. (2012) *Div. Planet. Sci. XXXXIV,* 209.03. [19] Schäfer, M., et al., (2014) *Icarus, 244,* 60-73. [20] Schultz, R.A., et al. (2006) *J. Struct. Geol., 28,* 2182-2193. [21] Marchi, S., et al. (2012) *Science, 336,* 690-694. [22] Schenk, P.M., et al. (2012) *Science, 336,* 694-697. [23] O'Brien, D.P., et al. (2014) *Planet. Space. Sci., 103,* 131-142. [24] Schmedemann, N., et al. (2014) *Planet. Space Sci., 103,* 104-130. [25] Yin, A. (2000) *J. Geophys. Res., 105,* 21475-21759. [26] Soliva, R., et al. (2006) *J. Geophys. Res., 111,* B01402. [27] Montési, L.G.J. and Zuber, M.T. (2003) J. Geophys. Res., 108, B22110. [28] Spudis, P.D. (1993) *Cambridge University Press.* [29] Moore, J.M., et al. (2004) *Icarus, 171,* 421-443. [30] Buczkowski, D.L., et al. (2008) *Icarus, 193,* 39-52. [31] Thomas, N., et al. (2012) *Planet. Space Sci., 66,* 96-124.

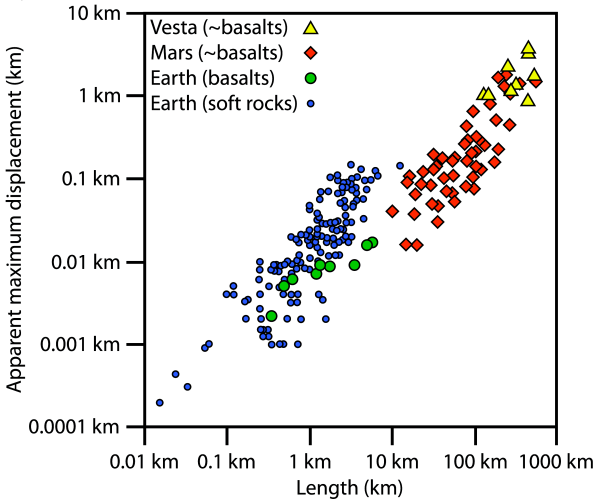

Figure. Plot of apparent maximum displacement versus length of faults on Vesta, Mars and Earth (adapted from [20]).